View metadata, citation and similar papers at core.ac.uk
brought to you by CORE
provided by Digital.CSIC

Expansion dynamics of the plasma produced by laser ablation of $BaTiO_3$ in a gas environment

J. Gonzalo,[a] C. N. Afonso,[b] and I. Madariaga
Instituto de Optica, CSIC, Serrano 121, 28006 Madrid, Spain

(Received 23 July 1996; accepted for publication 3 October 1996)

The expansion dynamics of the plasma produced by excimer laser ablation of $BaTiO_3$ has been studied by spatially resolved optical emission spectroscopy over a broad gas pressure range (10^{-7}–40 mbar), the gas being either reactive (oxygen) or inert (argon). The results obtained in both environments are qualitatively similar and they show that there is a distance-related pressure threshold above which the expansion dynamics differ from that of the free-expansion regime observed in vacuum. Analysis of the results in the framework of the drag model as well as the shock wave model show that the plasma expansion can be well described by the drag model for the initial stages of the expansion, whereas a delayed shock wave model is required for long distances to the target or high gas pressure. © *1997 American Institute of Physics.* [S0021-8979(97)02302-5]

INTRODUCTION

Ferroelectric materials are very attractive for different technological applications such as nonvolatile random access memories, capacitors, surface acoustic wave devices, and nonlinear optical devices, among others.[1] Many ferroelectrics, including $BaTiO_3$, have a perovskite-type crystalline structure that is similar to that of the high-T_c superconductors (HTSC).[1,2] The success of pulsed laser deposition in producing HTSC films has, thus, heightened the interest in using this technique to produce films of materials with similar structure, such as ferroelectrics.[3]

The plasma expansion dynamics produced by laser ablation of HTSC targets has been widely studied.[4–9] These studies have shown that parameters such as the laser energy density or the gas pressure determine the nature,[6,10,11] kinetic energy,[7–9,12] and distribution of species reaching the substrate,[12,13] thus, influencing the morphology, homogeneity, and crystalline characteristics of the deposited films.[13–15] Similar results have already been reported for $BaTiO_3$ films, since the ferroelectric response, the refractive index, the composition, and the crystalline orientation of the films have been found to depend on the laser energy density and oxygen pressure.[2,16–18] Therefore, the study of the influence of the gas pressure on the plasma expansion dynamics is an important issue to determine the optimum growth conditions for $BaTiO_3$ films.

In an earlier work,[18] we have reported that the change observed in the refractive index of $BaTiO_3$ films grown at gas pressures above 10^{-1} mbar was related to a change in the plasma expansion dynamics for target–substrate distances greater than the plume length. The aim of this work is, thus, to analyze the expansion dynamics of the plasma generated by laser ablation of a $BaTiO_3$ target in the presence of either a reactive (O_2) or inert (Ar) gas over a wide pressure range (10^{-7}–40 mbar). The nature and velocity of the species ejected from the target have been studied by spatially resolved real-time emission spectroscopy. The results are analyzed in the framework of the drag and shock wave models, with the range of validity of both models being discussed.

EXPERIMENT

Laser ablation of $BaTiO_3$ has been carried out using an ArF excimer laser ($\lambda=193$ nm, $\tau=12$ ns full width at half-maximum). The target is mounted in a rotating holder and placed in a vacuum chamber evacuated to a residual pressure of 10^{-7} mbar. The laser beam is focused on the surface of the target at an incidence angle of 45° giving a laser energy density of 2 J/cm^2. In order to study the influence of gas pressure on the plasma expansion dynamics, either oxygen or argon is dynamically allowed in the chamber up to pressures of 40 mbar.

The plasma formed during the laser ablation process is analyzed by means of spatially resolved real-time emission spectroscopy in the spectral range 380–620 nm and at different distances from the target (0–20 mm). The plasma emission is imaged onto the entrance slit of a SPEX spectrometer with magnification of $\times 2$. Depending on the distance to the target (d), two different slit widths were considered in order to improve the signal-to-noise ratio. The resulting spectral and spatial resolutions were: 0.03 nm and 60 μm for $d<14$ mm and 0.1 nm and 130 μm for long distances. As has been described elsewhere,[8,13,19] the light emitted is collected by a photomultiplier (15 ns rise time) that is connected to a boxcar averager for spectrum recording, or to a 500 MHz digitizer for transient emission measurements.

RESULTS

Figure 1 shows an emission spectrum recorded in vacuum at a distance of 2.4 mm from the target. There are a larger number of lines, most of them related to neutrals (Ba*, Ti*) and ions (Ba^+*,Ti^+*). No emission from oxidized species could be detected under any of the conditions studied, although emission from BaO* and TiO* was very carefully looked for since the presence of these species has been re-

[a]Present address: Dept. of Applied Physics, University of Hull, HU6 7RX, Hull, UK.
[b]Electronic mail: cnafonso@pinarl.csic.es

Downloaded¬24¬Feb¬2010¬to¬161.111.180.191.¬Redistribution¬subject¬to¬AIP¬license¬or¬copyright;¬see¬http://jap.aip.org/jap/copyright.jsp

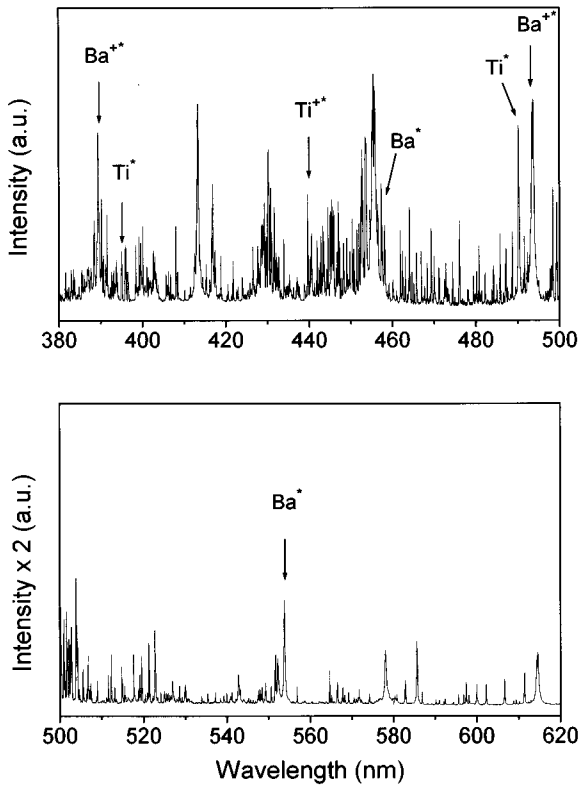

FIG. 1. Emission spectrum of the plasma produced by laser ablation of $BaTiO_3$ in vacuum (10^{-7} mbar) recorded at a distance of 2.4 mm from the target surface. The transitions marked with an arrow are those studied in this work.

ported during laser ablation of YBaCuO (Refs. 4, 6, 10, and 11) and Ti:Al_2O_3 (Ref. 20), respectively. The emission lines are identified according to standard tabulations[21] and those studied on this work are marked with an arrow in Fig. 1. 'Table I summarizes the emission lines studied in this work, along with the electronic transition responsible for their presence and the lifetime of the excited state.[22] A strong contribution from the continuum emission overlaps that of the excited species in the neighborhood of the target ($d<0.5$ mm). This contribution has been reported during ablation of several materials and it disappears when increasing the distance from the target.[7,8,19] Figure 2 shows emission transients corresponding to the emission line at 553.6 nm (Ba*) recorded at a distance of 4 mm from the target in different environments: vacuum, 1 mbar of oxygen and 20 mbar of oxygen. It is clearly seen that the presence of an atmosphere has a

TABLE I. Electronic transition, lifetime, and species responsible for the emission lines studied in this work.

Specie	Wavelength	Transition	Lifetime (ns)
Ba^{+}*	389.2	$6d\ ^2D_{3/2}\rightarrow 6p\ ^2P^0_{1/2}$	6
Ti*	394.9	$y\ ^3D^0_{1/2}\rightarrow a\ ^3F_2$	20
Ti^{+}*	439.5	$z\ ^2F_{7/2}\rightarrow a\ ^2D_{5/2}$	106
Ba*	458.0	$6p^2\ ^1D_2\rightarrow 6p\ ^3P^0_2$	14
Ti*	490.0	$y\ ^3H^0_5\rightarrow a\ ^3G_4$	···
Ba^{+}*	493.4	$6p\ ^2P^0_{1/2}\rightarrow 6s\ ^2S_{1/2}$	10
Ba*	553.6	$6p\ ^1P^0_{1/2}\rightarrow 6s^2\ ^1S_0$	8

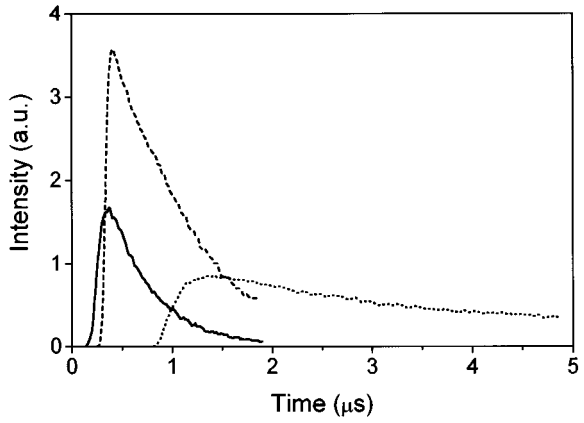

FIG. 2. Emission intensity transients from the Ba* emission line at 553.6 nm recorded at $d = 4$ mm from the target surface in (—) vacuum, (--) 1 mbar of O_2 and (····) 20 mbar of O_2.

strong influence on the observed emission. Both the emission intensity maximum (I_M) and the time at which this maximum is observed (t_M) are pressure dependent. Moreover, increasing the gas pressure also produces a broadening of the emission transients.

The dependence of I_M and t_M on the oxygen pressure for the line at 553.6 nm (Ba*) are shown in Figs. 3(a) and 3(b),

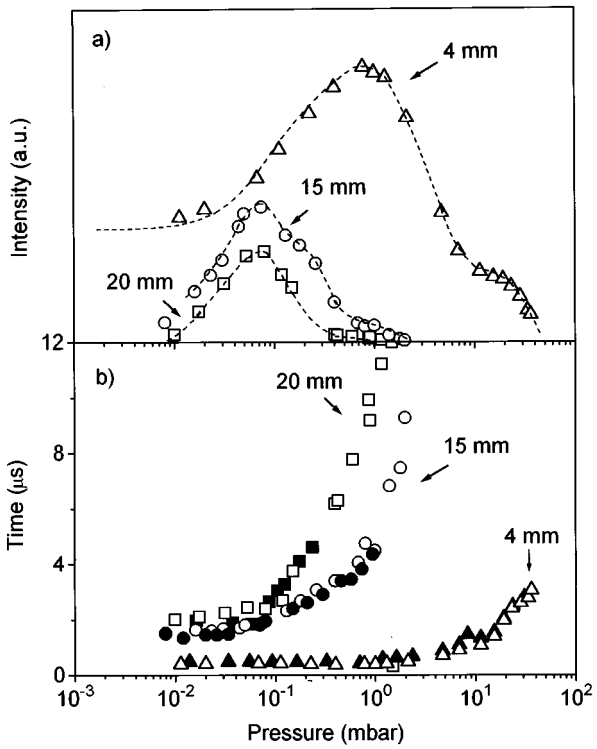

FIG. 3. (a) Maximum emission intensity (I_M) and (b) its delay with respect to the laser pulse (t_M) as a function of the oxygen pressure applied. The results are recorded at distances of (△, ▲) 4 mm, (○, ●) 15 mm, and (□, ■) 20 mm from the target surface and correspond to (■, ●, ▲) the Ba^{+}* emission line at 493.4 nm and to (□, ○, △) the Ba* emission line at 553.6 nm. The intensity recorded at 4 mm cannot be directly compared to that recorded at 15 and 20 mm since it has been recorded with a higher resolution.

Downloaded¬24¬Feb¬2010¬to¬161.111.180.191.¬Redistribution¬subject¬to¬AIP¬license¬or¬copyright;¬see¬http://jap.aip.org/jap/copyright.jsp

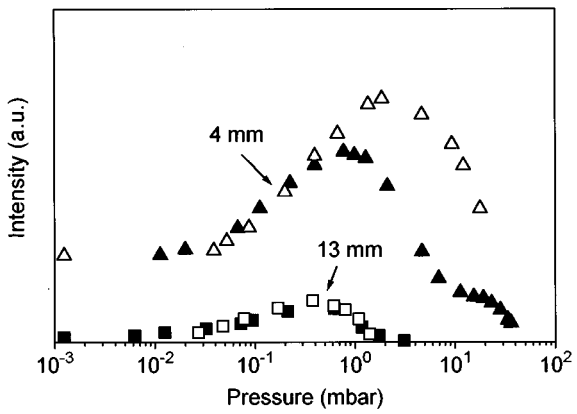

FIG. 4. Maximum emission intensity (I_M) of the Ba* emission line at 553.6 nm as a function of the gas pressure applied. Results are recorded either in (▲, ■) oxygen or (△, □) argon at distances of 4 and 13 mm from the target surface.

respectively, for three distances from the target: 4, 15, and 20 mm. Note that the high I_M values for 20 and 15 mm are not in the same scale than those for 4 mm, since in the former two cases it was necessary to increase the width of the spectrometer slit to improve the signal-to-noise ratio. In all cases, I_M increases with oxygen pressure up to a maximum value that depends on the distance from the target, and then decreases sharply to zero for higher pressures. Both the pressure at which the maximum of I_M is observed and that at which I_M becomes zero depend on the distance from the target; the higher the distance the lower the pressure. Figure 3(b) shows that t_M remains constant and close to the value obtained in vacuum, up to a pressure threshold that again depends on the distance to the target. For pressures above this threshold, t_M increases sharply, this increase being consistent with the reduction in the ejected species velocity that has been widely reported in the literature in the presence of a gas environment.[4,5,7–9,12] Figure 3(b) includes the t_M values not only for the emission line at 553.6 nm (Ba*), but also for that at 493.4 nm (Ba^+*). It is clearly seen that the results are very similar for both species, with the same results observed both for the maximum emission intensity curve, which is not shown in Fig. 3(a), and for the other species studied.

The influence of the gas pressure on I_M and t_M for the different emission lines considered in Table I has been also studied in an argon environment. The results obtained in argon and oxygen show similar features as can be seen in Fig. 4, where the dependence of I_M on the gas pressure for both argon and oxygen is shown for the emission line at 553.6 nm (Ba*) at 4 and 13 mm from the target. Although the emission is detected over a similar pressure range for the two gas environments, the relative increase of I_M with respect to the emission detected in vacuum depends on the nature of the gas, this increase being higher in argon than in oxygen. This result is similar to that reported earlier during laser ablation of HTCS.[8]

Figure 5 shows the dependence of the distance (d) from the target at which the maximum emission intensity (I_M) occurs on the delay of this maximum with respect to the laser pulse (t_M). The data have been collected for the emission

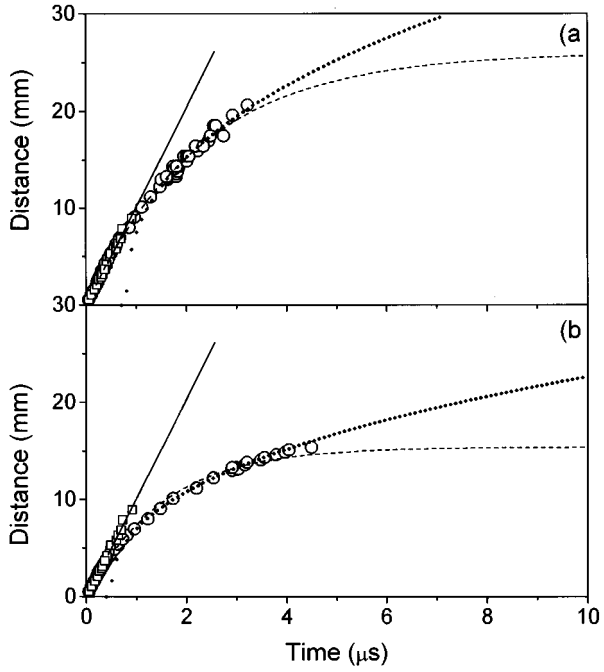

FIG. 5. Distance at which the maximum emission intensity (I_M) from the Ba^+* emission line at 493.4 nm is observed as a function of its delay with respect to the laser pulse (t_M). Results were collected in (a) 10^{-1} mbar and (b) 1 mbar of oxygen pressure. The results obtained in vacuum (□) are also included for comparison. The dashed line (--) shows the best fit obtained using the drag model [$d = d_f[1 - \exp(-\beta t)] - d_0$, with d_f=26 mm, β=0.45 μs^{-1}, d_0=0.1 mm for 10^{-1} mbar, and d_f=15 mm, β=0.67 μs^{-1}, d_0=0.0 mm for 1 mbar]. The dot line ($\cdots$) shows the best fit achieved with the delayed shock wave model [$d = k'(t - t_s)^{2/5} - d_0$, with $k' = (k/p)^{1/5}$ and $k' = 1.42$, t_s=0.80 μs, d_0=0.3 mm for 10^{-1} mbar and $k' = 0.92$, $t_s = 0.49$ μs, $d_0 = 0.3$ mm for 1 mbar]. The full line shows the free-expansion regime.

line at 493.4 nm (Ba^+*) in an oxygen pressure of 10^{-1} mbar [Fig. 5(a)] and 1 mbar [Fig. 5(b)]. The results obtained in vacuum are also included for comparison and they show a linear dependence over the whole range of distances for which emission could be detected. When an oxygen pressure is applied, the emission can be detected at greater distances (~20 mm) and higher delays (~5 μs) than in vacuum (~10 mm and 1 μs). The dependence is no longer linear for distances $d > 10$ mm at an oxygen pressure of 10^{-1} mbar, or at shorter distances for higher pressures. Similar features are observed for the other emission lines studied or when the gas was changed to argon. The velocities calculated from the slope (d/t_M) in the linear region are in the range 10–13 $\times 10^5$ cm/s for neutrals and 13–14 $\times$ 10^5 cm/s for ions. The results obtained in a gas pressure are, thus, consistent with a slowing down of the ejected species due to interactions with the gas species as has been pointed out above and widely reported.

DISCUSSION

The results presented here clearly show that the plasma expansion dynamics are strongly affected by the presence of a gas environment. The emission intensity (I_M) increases significantly above a pressure threshold and is independent

Downloaded¬24¬Feb¬2010¬to¬161.111.180.191.¬Redistribution¬subject¬to¬AIP¬license¬or¬copyright;¬see¬http://jap.aip.org/jap/copyright.jsp

of the reactive or inert character of the gas environment [Figs. 3(a) and 4]. The lifetime (τ) of the excited states studied, shown in Table I, is always of the order of tenths of ns while the time at which the maximum emission is observed (t_M) in the presence of a gas environment is of the order of a few μs [Fig. 3(b)]. Since $\tau \ll t_M$, the observed intensity increase for pressures above a threshold value has to be related to species that have been excited during the plasma expansion due to either collisional excitations or to electron-impact excitation or to recombination.[8,23,24] The ionization of the gas species provides the necessary free electrons to promote excitation phenomena, and thus, an increase in the emission intensity.[12,24] Nevertheless, the emission intensity decreases above a pressure threshold that depends on the distance from the target. This behavior has been observed before[23,24] and has been attributed to different processes such as electron impact ionization of metastable species ($A^* + e^- \rightarrow A^+ + 2e^-$), collisional quenching ($A^* + M_{\text{slow}} \rightarrow A^+ + M_{\text{fast}}$) (Refs. 12 and 23), or the confinement of the plasma to a limited region at high gas pressures.[6,8,24] The former two processes lead to the formation of ionized species and should induce an increase in their emission intensity that is not experimentally observed. The latter process is, therefore, more likely and is in good agreement with the sharp increase of t_M observed at high gas pressures [Fig. 3(b)]. If we assume that the amount of material ejected per pulse does not depend on the gas pressure, the observed increase of t_M suggests that the plasma expands more slowly at high pressures. The density of the plasma is, thus, increased in the region close to the target, promoting the confinement of the plasma. If the pressure is high enough, this confinement will become more evident and will be limited to a finite region close to the target; therefore, the emission observed at longer distances from the target would tend to disappear. This reasoning is in very good agreement with the behavior observed experimentally and shown in Fig. 3(a): when the pressure increases, the density of excited species (related to I_M) at long distances (i.e., 20 mm) is much lower than at short distances (i.e., 4 mm). For the highest pressure (40 mbar), the plasma has been confined to distances from the target of less than 4 mm, and consequently, no emission is detected even at this distance.

The sharp increase of t_M above a threshold of pressure [Fig. 3(b)] or distance (Fig. 5) is a clear indication that the plasma expansion dynamics in the presence of a gas change with respect to the free-expansion dynamics followed in vacuum or for low pressures/short distances.[4,5,7,8,24] Under these conditions, the plasma expansion process in a gas environment has been analyzed in terms of different models depending on the pressure range. For the early stages of expansion and at low pressures (<1 mbar), a drag model has been considered,[7] which accounts for the scattering of the ejected species by the gas atoms or molecules.[7,8,10,12] In this model, the ejected species are considered as an ensemble that experiences a viscous force proportional to its velocity. The distance d from the target surface can be expressed as a function of the time t at which the maximum of the transient emission is observed according to the following equation:[5,7,25]

$$d = d_f[1 - \exp(-\beta t)] - d_0, \tag{1}$$

where β is the slowing coefficient, d_f is the stopping distance of the plume, and d_0 is a boundary condition to take into account the fact that it is necessary to wait a certain time interval, of the order of the lifetime of the excited state, before emission occurs at $d = 0$ (Ref. 8). The best fits to the experimental results shown in Fig. 5 are also included in Fig. 5, and it is clearly seen that the agreement is excellent for the initial states. For a pressure of 1 mbar [Fig. 5(b)] and for times longer than 4 μs, the drag model predicts distances slightly shorter than those observed experimentally. The stopping distance (or length) of the plume obtained from this model is 26 or 15 mm for oxygen pressures of 10^{-1} or 1 mbar, respectively. These results are nevertheless in contradiction with the experimental results reported in the literature,[2,16,18] which show that $BaTiO_3$ films can be grown under similar experimental conditions on substrates located at distances to the target larger than $\sim$26 mm.

At higher pressures, the formation of a blast wave has been observed.[4,5,25] Under these conditions the shock wave model describes well the plasma expansion for a limited range of distances that depend on the gas pressure[4,5,7] and is determined by (a) the distance from the target at which the mass of the gas displaced by the ejected material is much higher than the mass of the ejected material and (b) the distance from the target at which the plasma pressure becomes similar to the pressure of the gas environment. The expression for the shock wave is

$$d = (k/p)^{1/5} t^{2/5} - d_0, \tag{2}$$

where d, d_0 and t denote the same parameters as in (1), k is a constant proportional to the laser energy density, and p is the gas pressure. If one takes into account that the shock wave model can strictly be applied only after the mass of the gas surrounding the shock wave is higher than the mass of the ablated material[5,7] (i.e., a time t_s after the laser pulse), a delayed shock wave should be considered as has been suggested elsewhere.[25] In this case, the expression for the shock wave becomes

$$d = (k/p)^{1/5} (t - t_s)^{2/5} - d_0 \tag{2a}$$

where all the symbols denote the same parameters as in Eq. (2) and t_s is the boundary condition for the delayed shock wave. The delayed shock wave model fits the experimental results shown in Fig. 5 very well for times above thresholds of 0.80 and 0.49 μs for oxygen pressures of 10^{-1} and 1 mbar, respectively. Extrapolating the simulations to long distances/times, it is clearly seen that the shock wave model predicts an increasing function that is in contrast to the tendency to saturation predicted by the drag model. There is, thus, no limit to the plume length within the framework of the delayed shock wave model for pressures of 10^{-1} mbar, which is consistent with the results obtained during the growth of the $BaTiO_3$ films mentioned above.[2,16,18]

A comparison of the fit of the experimental results to the two models considered shows clearly that the drag and shock wave models are valid for the initial and final stages of the expansion dynamics, respectively, with an intermediate

Downloaded¬24¬Feb¬2010¬to¬161.111.180.191.¬Redistribution¬subject¬to¬AIP¬license¬or¬copyright;¬see¬http://jap.aip.org/jap/copyright.jsp

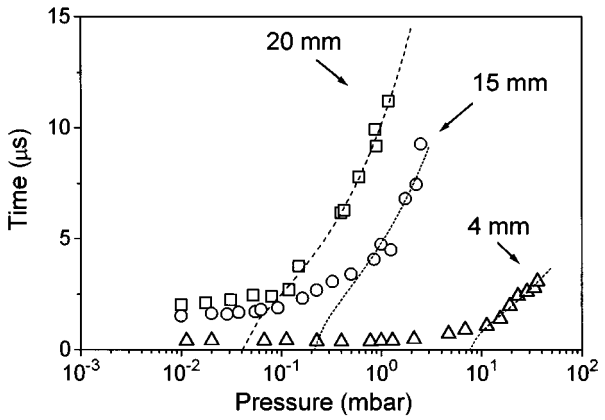

FIG. 6. Delay of the maximum emission intensity with respect to the laser pulse (t_M) as a function of the oxygen pressure applied measured from the Ba* emission line at 553.6 nm at (△) 4 mm, (○) 15 mm, and (□) 20 mm from the target surface. The dashed line (--) shows the fit of the experimental results obtained with the delayed shock wave model [$t = k''(p - p_s)^{1/2}$, with $k'' = (d^5/k)^{1/2}$, and $k'' = 0.54$, p_s=7.97 mbar for 4 mm, $k'' = 5.48$, p_s=0.23 mbar for 15 mm, and $k'' = 10.39$, p_s=0.04 mbar for 20 mm].

distance/time interval existing in which both models fit the experimental results reasonably well. The limits of applicability of each model and the common interval in which both models can be applied clearly depend on the gas pressure.

The sharp increase of t_M shown in Fig. 3(b) suggested a change in the plasma expansion dynamics that depends on the relationship between the pressure and the distance from the target. There is a first pressure interval seen in Fig. 3(b) in which the values of t_M show only a slight increase with pressure (i.e., pressures lower than 5 mbar for $d=4$ mm). For higher pressures, a sharp increase of t_M is observed and, therefore, it is for these high pressures for which the shock wave model most likely applies. From Eq. (2), it is then possible to obtain the dependence of t_M on pressure for a fixed distance[5,8]

$$t=(d^5/k)^{1/2}(p-p_s)^{1/2}, \tag{3}$$

where all the symbols denote the same parameters as in (2), d_0 has been neglected since $d_0 \ll d$, and the term p_s has been introduced to account for the pressure threshold above which the shock wave is observed at the distance d from the target. Figure 6 shows both the experimental results obtained for the emission line at 553.5 nm (Ba*) and the theoretical fits achieved using Eq. (3). It is clearly seen that the shock wave model fits the experimental results very well above the distance-related pressure thresholds (p_s), which decrease as the distance from the target increases (compare p_s=8 mbar at 4 mm to 4×10^{-2} mbar at 20 mm). It can, thus, be concluded that the shock wave model describes very well the existence of distance-related pressure thresholds above which the delays diverge from those observed in the free-expansion regime occurring in vacuum.

CONCLUSIONS

The comparison of the emission spectra obtained during the ablation of $BaTiO_3$ in vacuum, oxygen, and inert argon shows the same emission lines, the change in their intensity being the only new feature observed. A distance-related pressure threshold is observed above which a decrease of the emission intensity and a slowing down of the ejected species takes place, thus, suggesting a confinement of the plasma to regions close to the target for high pressures.

The slowing down of the ejected species has been analyzed within the framework of the drag and shock wave models. It is concluded that the drag model describes well the early stages of the expansion dynamics (short distances) whereas a delayed shock wave model is required for the final stages (large distances), the distance range of applicability of each model being pressure dependent. Moreover, the delayed shock wave model is also appropriate to describe the slowing down of the ejected species above the distance-related pressure threshold.

ACKNOWLEDGMENTS

Dr. J. Perrière (GPS, Univ. de Paris VI et VII, France) is thanked for providing the target. This work has been partially supported by CICYT (Spain) under TIC 96-0467 project. Two of the authors, J. Gonzalo and I. Madariaga acknowledge a FPI grant from the Spanish Ministry of Educación y Ciencia and an ''Introducción a la Investigación'' grant from CSIC, respectively.

[1] R. E. Leucthner and K. S. Grabowski, *Pulsed Laser Deposition of Thin Films*, edited by D. B. Chrisey and G. K. Hubler (Wiley, New York, 1994), p. 473.
[2] D.-Y. Kim, S.-G. Lee, and Y.-K. Park, Jpn. J. Appl. Phys. 1 **34**, L1564 (1995).
[3] K. L. Saenger in Ref. 1, p. 582, and references therein.
[4] P. E. Dyer, A. Issa, and P. H. Key, Appl. Phys. Lett. **57**, 186 (1990).
[5] W. K. A. Kummudumi, Y. Nakayama, Y. Nakata, T. Okada, and M. Maeda J. Appl. Phys. **74**, 7510 (1993).
[6] H. F. Sakeek, T. Morrow, W. G. Graham, and D. G. Walmsley, J. Appl. Phys. **75**, 1140 (1994).
[7] D. B. Geohegan, in Ref. 1, p. 115.
[8] J. Gonzalo, F. Vega, and C. N. Afonso J. Appl. Phys. **77**, 6588 (1995).
[9] K. Fukushima, Y. Kanle, and T. Morishita, J. Appl. Phys. **74**, 6948 (1993).
[10] A. Gupta, J. Appl. Phys. **73**, 7877 (1993).
[11] H. S. Kwok, Thin Solid Films **218**, 277 (1992).
[12] K. L. Saenger, Proc. Adv. Mater. **3**, 63 (1993).
[13] J. Gonzalo, C. N. Afonso, F. Vega, D. Martinez García, and J. Perrière, Appl. Surf. Sci. **86**, 40 (1995).
[14] M. C. Foote, B. B. Jones, B. D. Hunt, J. B. Barner, R. P. Vasquez, and L. Bajuk, Physica C **201**, 176 (1992).
[15] H. M. Bedekar, A. Safari, and W. Wilber Physica C **202**, 42 (1992).
[16] T. Okada, Y. Nakata, H. Kaibara, and M. Maeda, Jpn. J. Appl. Phys. 1 **134**, L1536 (1995).
[17] R. Gómez San Román, R. Pérez Casero, A. Laurent, J. Perrière, P. Gergaud, and J. L. Lebrun, J. Appl. Phys. (submitted).
[18] J. Gonzalo, C. N. Afonso, and J. M. Ballesteros, Appl. Surf. Sci. (accepted).
[19] F. Vega, C. N. Afonso, and J. Solís, J. Appl. Phys. **73**, 2472 (1993).
[20] P. E. Dyer, S. R. Jackson, P. H. Key, W. J. Metheringham, and M. J. J. Schmidt, Appl. Surf. Sci. **96–98**, 849 (1996).
[21] W. F. Heggers, C. H. Corliss, and B. F. Scribner, NBS Monograph **145** (1975); in *Handbook of Chemistry and Physics*, 75th ed., edited by R. Lide (CRC Press, Florida, 1994).
[22] C. E. Moore, NSRDS-NBS Monograph **35** (1975); G. A. Martin, J. R. Fuhr, and W. L. Wiese, J. Phys. Chem. Ref. Data **17**, Suppl. 3 (1988).
[23] C. Timmer, S. K. Srivastava, T. E. Hall, and A. Fucaloro, J. Appl. Phys. **70**, 1888 (1991).
[24] H. P. Gu, Q. H. Lou, N. H. Cheung, S. C. Chen, Z. Y. Wang, and P. K. Lin, Appl. Phys. B **58**, 143 (1994).
[25] M. Okoshi, T. Yoshitake, and K. Tsushima, Appl. Phys. Lett. **63**, 3340 (1994).

Downloaded¬24¬Feb¬2010¬to¬161.111.180.191.¬Redistribution¬subject¬to¬AIP¬license¬or¬copyright;¬see¬http://jap.aip.org/jap/copyright.jsp